Exosomal microRNA-486-5p From Adipose Derived Stem Cells Alleviate Chondrocyte Apoptosis and Osteoarthritis by Attenuating Endoplasmic Reticulum Stress

Yiming Wang
Tongji University School of Medicine
Aoyuan Fan
Tongji University School of Medicine
Liangyu Lu
Tongji University School of Medicine
Zhangyi Pan
Tongji University School of Medicine
Min Ma
Tongji University School of Medicine
Shulin Luo
Tongji University School of Medicine
Zheng Liu
Tongji University School of Medicine
Liqing Yang
Tongji University School of Medicine
Junfeng Cai
Tongji University School of Medicine
Feng Yin (001yinfeng@sina.com)
Tongji University School of Medicine https://orcid.org/0000-0002-2070-0085

Research

Keywords: Exosomes, adipose derived stem cells, microRNA-486-5p, osteoarthritis, endoplasmic reticulum stress

Posted Date: September 21st, 2021

DOI: https://doi.org/10.21203/rs.3.rs-910465/v1

Exosomal microRNA-486-5p from adipose derived stem cells alleviate chondrocyte apoptosis and osteoarthritis by attenuating endoplasmic reticulum stress

Yiming Wang[1]*, Aoyuan Fan[1]*, Liangyu Lu[1], Zhangyi Pan[1], Min Ma[1], Shulin Luo[1], Zheng Liu[1], Liqing Yang[1], Junfeng Cai[1#], Feng Yin[1#]

[1]Department of joint surgery, Shanghai East Hospital, Tongji University School of Medicine, Shanghai, China.

* These authors contributed equally to this article.

[#]Corresponding author: Feng Yin, Department of joint surgery, Shanghai East Hospital, Tongji University School of Medicine, Shanghai, China. E-mail: 001yinfeng@sina.com

Co-corresponding author: Junfeng Cai, Department of joint surgery, Shanghai East Hospital, Tongji University School of Medicine, Shanghai, China. E-mail: dr_cjf@163.com

Abstract

Background: As one of the most common disabling diseases in the musculoskeletal system, osteoarthritis (OA) is characterized with cartilage matrix degeneration and chondrocyte apoptosis. Endoplasmic reticulum (ER) stress is well known for participate in chondrocyte apoptosis and cartilage degeneration in OA progression. microRNAs

(miRNAs) could function in cartilage homeostasis, yet limited is known regarding whether miRNA could modulate ER stress in chondrocytes. Here, we reported that exosomal microRNA-486-5p from adipose derived stem cells (ADSCs) could alleviate chondrocyte apoptosis and osteoarthritis by attenuating ER stress

Methods: ER stress markers and inflammatory cytokines were analyzed in OA knee joint by immunohistochemistry and immunofluorescence staining. IL-1β induced apoptosis of chondrocytes was analyzed using flow cytometry. ER stress markers and inflammatory cytokines of IL-1β induced chondrocytes were analyzed by immunofluorescence staining, western blot and ELISA. miR-486-5p mimic overexpressed ADSCs and their exosomes were validated and used to treat IL-1β induced chondrocytes together with miR-486-5p mimic. Different administrative methods of miR-486-5p mimic were tracked both in vitro and in vivo, and further used to treat OA model mice. OA progression of mice was analyzed by H&E, safranin O/fast green, immunofluorescence and immunohistochemistry staining.

Results: We validated the increased inflammation and ER stress in OA synovium and cartilage, and the IL-1β induced chondrocyte apoptosis was through the ER stress activation. Administration of exogenous miR-486-5p could not only inhibit the ER stress, but also alleviate chondrocytes apoptosis and promote matrix regeneration. In comparison with direct administration of miR-486-5p and miR-486-5p overexpressing ADSCs, exosomes seem to be a better delivery vehicle for miRNA in modulating chondrocyte homeostasis. Our immunofluorescence and IVIS imaging data further validated the better delivery ability of exosomes through tracking the uptake of miR-

486-5p in chondrocytes and the diffusion of miR-486-5p in the knee joint with different transportation methods. Exosomal microRNA-486-5p also showed a better effect on alleviating mice OA.

Conclusion: Our data demonstrated that exosomes are better delivery vehicle for miR-486-5p on alleviating chondrocyte apoptosis and osteoarthritis. This study provides evidence to this efficient strategy of exosomal miRNA delivery and to the miRNA-based therapy for OA.

Keyword: Exosomes, adipose derived stem cells, microRNA-486-5p, osteoarthritis, endoplasmic reticulum stress

Background

Osteoarthritis (OA) is characterized by articular cartilage degradation, which is largely induced by the inflammatory microenvironment of the entire joint (1). Inflammatory cytokines in the OA joint can activate prolonged endoplasmic reticulum (ER) stress in chondrocytes, the major resident cell of articular cartilage, causing apoptosis (2). Inhibiting the ER stress-induced apoptosis of chondrocytes holds the potential to become a novel OA therapy.

MicroRNAs (miRNAs) are clusters of small noncoding RNAs that suppress gene expression through binding to the 3'-untranslated regions (3'-UTRs) region of the targeted mRNAs. miRNAs have emerged as a double-edged sword during the interaction with ER stress as some of them can either suppress (3) or promote (4) ER

stress. However, whether and which miRNAs could regulate ER stress in chondrocytes remain poorly studied. Li et al. (5) reported that miR-375 could suppress autophagy and promote ER stress in chondrocytes, and the inhibition of miR-375 could attenuate OA symptoms. Yet to our knowledge, no other study has been published to clarify other miRNAs that could regulate ER stress in chondrocytes. miR-486-5p has been previously investigated in oncology and it is an important biomarker in cancer diagnosis and prognosis (6, 7). Recent studies have shown that the expression level of miR-486-5p is related to many musculoskeletal diseases including intervertebral disc degeneration, knee OA and rheumatoid arthritis (8-10). Moreover, miR-486-5p was identified to participate in the regulation of apoptosis in nucleus pulposus cells (11). However, delivery of miR-486-5p in previous studies was through the over-expression of miR-486-5p in autologous cells by direct genetic manipulation, posing a potential risk of biological safety. Direct administration is another potential delivery method of miRNAs, but poor serum stability and low cellular uptake of the direct delivered miRNAs have remarkably restrained their clinical application (12). More effective and safer administration method is in urgent need to meet clinical requirements.

Mesenchymal stem cells (MSCs) are innovative therapeutics of OA originally based on their chondrogenic differentiation ability. Recently, it has been demonstrated that the paracrine factors including exosomes (exos), also contributes to the MSC-based OA therapy (13). Exos are subpopulation of nanoscale extracellular vesicles involved in intercellular communication, in which contain various molecules including proteins, lipids, and a variety of RNAs (miRNAs, messenger RNAs, transfer RNAs, etc.) (14).

MSCs-derived exos have been demonstrated to benefit cartilage regeneration via increasing proliferation, diminishing apoptosis and regulating inflammatory activity (15, 16). Despite its original contents, exos are naturally capable of encapsulating and delivering cargo to modify cellular function, which emphasizes the potential usage as therapeutic delivery vehicles for miRNA-based therapy. Recent studies have indeed suggested that exos derived from both miR-92-3p and miR-140-5p-overexpressed MSCs are superior over the original MSC-derived exos for OA suppression (17, 18). However, it is still unclear whether exos are a better mode of conveyance when compared to the direct administration of miRNAs and MSCs.

Herein, we transduced miR-486-5p mimic into adipose derived stem cells (ADSCs) to acquire miR-486-5p mimic overexpressed ADSCs (miR-486-5p mimic ADSCs) and their exos (miR-486-5p mimic exos). We conduct a comprehensive comparison among miR-486-5p, miR-486-5p mimic ADSCs and miR-486-5p mimic exos regarding their role in chondrocyte apoptosis inhibition *in vitro* and OA alleviation *in vivo*. We believe this will provide new insight into the miRNA-cell interaction and the delivery methods of miRNAs on inhibiting chondrocytes apoptosis and OA progression.

Materials and Methods

This study was carried out in compliance with the Declaration of Helsinki.

Sample collection and cell preparation

Human subjects research was performed according to the Institutional Review Boards

111 at Shanghai East Hospital via approved protocols with appropriate informed consent.
112 Normal synovium samples were harvested from three patients underwent exploratory
113 arthroscopy who showed no radiographic changes of the knee joint and no obvious
114 cartilage lesion during arthroscopy (1 male and 2 female, 68 years old on average).
115 OA synovium and articular cartilage samples were harvested from three patient
116 underwent total knee arthroplasty (1 male and 2 female, 65 years old on average).
117 Wore weight bearing area articular cartilage was used as OA cartilage, and samples
118 collected from none-weight bearing area and showed no obvious abrasion under
119 stereoscope were considered as normal articular cartilage. Samples were fixed in
120 formaldehyde, dehydrated before embedding in paraffin. Cartilage samples were
121 additionally decalcified for three days before dehydration. Samples were cut into 5 μm
122 thick sections.
123 Subcutaneous adipose tissues were harvested from 3 volunteers (2 male and 1
124 female, 25 years old on average). The adipose tissues were minced and sequentially
125 digested with 0.1% collagenase II (Sigma-Aldrich, St. Louis, MO, USA) for 2 h and 0.1%
126 trypsin (Gibco, Carlsbad, CA, USA) for 0.5 h at 37 ℃ to separate cells. After filtration
127 and centrifugation, ADSCs were seeded in growth medium [Minimum Essential
128 Medium-Alpha Modification (α-MEM) containing 10% fetal bovine serum (FBS), 100
129 U/ml penicillin, 100 μg/ml streptomycin (Invitrogen, Carlsbad, CA)].
130 Human articular chondrocytes cell line was purchased from Sciencell (Catalog
131 #4650).
132 **Immunohistochemical and immunofluorescent staining**

For immunohistochemical staining, sections were deparaffinated, rehydrated and blocked before antibody staining. Sections were then incubated with primary antibodies against IL-1β (Affinity, AF5103), TNF-α (Affinity, AF7014), CHOP (Proteintech, 15204-1-AP), GRP78 (Proteintech, 11587-1-AP), iNOS (Proteintech, 18985-1-AP) and CD163 (Proteintech, 16646-1-AP) followed by the horseradish peroxidase (HRP)-conjugated Goat anti Rabbit secondary antibody (Aspen, AS-1107).

For immunofluorescent staining, sections were rehydrated and blocked before antibody staining. Sections or cells were then incubated with primary antibodies against iNOS (Proteintech, 18985-1-AP), CD163 (Proteintech, 16646-1-AP) or CHOP (Proteintech, 15204-1-AP), then followed by the Cy3-labeled Goat anti Rabbit secondary antibody (Aspen, AS-1109). Both sections and cells were stained with 4-6-diamidino-2-phenylindole (DAPI, Beyotime, China) for 5 min.

Images were acquired using Olympus IX51 Inverted Fluorescence Microscope (Olympus, Japan).

qPCR, western blot and ELISA

For qPCR, total RNA was extracted using TRIzol reagent (Invitrogen) and was reverse-transcribed using PrimeScript RT Reagent Kit (Takara, Japan). qPCR reaction was conducted in a final volume of 20 ul containing 10 ul of HieffTM qPCR SYBR Green Master Mix (YEASEN) and 2 ul of cDNA. qPCR amplification was performed using a 7500 real-time PCR System (APPLIED Biosystems) according to the manufacturer's instructions. miR-486-5p level was analyzed and normalized by U6. mRNA level of

COL2A1, *ACAN* and *MMP13* were assessed and *GAPDH* was used as the internal control. The PCR primers used include hsa-miR-486-5p (MIMAT0002177): 5'- TGT ACT GAG CTG CCC CGA G-3' and 5'- CTC AAC TGG TGT CGT GGA GTC-3'; U6 (NR_004394.1): 5'- CTC GCT TCG GCA GCA CAT-3' and 5'- AAC GCT TCA CGA ATT TGC GT-3'; GAPDH (NM_001256799.2): 5'- CAT CAT CCC TGC CTC TAC TGG-3' and 5'- GTG GGT GTC GCT GTT GAA GTC-3'; ACAN (NM_013227.3): 5'- AAG GGC GAG TGG AAT GAT GT-3' and 5'- CGC TTC TGT AGT CTG CGT TTG T-3'; COL2A1 (NM_001844.4): 5'- ATG CCA CAC TCA AGT CCC TCA-3' and 5'- GTC TCG CCA GTC TCC ATG TTG-3'; MMP13 (NM_002427.4): 5'- ATC ATG ATC TCT TTT GGA ATT AAG G-3' and 5'- AAC AAG TTG TAG CCT TTG GAA CTA C-3'.

For western blot analysis, total protein was extracted from cell lysis using protein extraction kit (Byotime) and 20 μg of total protein from each sample were separated using NuPAGE™ Bis-Tris Mini Gels (Invitrogen) in the XCell SureLock™ Mini-Cell (Life Technologies, Carlsbad, CA). Bands were transferred onto a nitrocellulose membrane using an XCell II™ Blot module (Life Technologies) at 70 V at 4°C overnight. After blocking, the membrane was incubated with primary monoclonal antibodies targeting p-PERK (bioss, bs-330R), PERK (Cell signaling technology, #3192), p-IRE1α (abcam, ab48187), IRE1α (Cell signaling technology, #3294), SOX9 (santa, sc-166505), GRP78 (Cell signaling technology, #3183), type II collagen (Proteintech, 28459-1-AP), MMP13 (abcam, ab39012), cleaved Caspase-3 (abcam, ab49822) and GAPDH (abcam, ab37168) in 5% BSA in TBST buffer at 4°C overnight, followed by the secondary antibody of HRP-conjugated goat anti-rabbit (Aspen, AS-1107) for 1 h.

ECL™ Prime Western Blotting Detection Reagents (Amersham Biosciences, Waltham, MA) were used for exposure.

The secretion of inflammatory cytokines including IL-1β and TNF-α by chondrocytes were evaluated using human ELISA kit (ELK Biotechnology, ELK1156 and ELK1190). Cell free supernatant was collected after centrifugation at 2000g for 10min. ELISA analysis was conducted according to the manufacturer's instruction.

Apoptosis and proliferation analysis

Apoptosis was measured by flow cytometry using a FITC-conjugated Annexin V and propidium iodide (PI) apoptosis kit (Invitrogen) based on the manufacturer's instructions. Briefly, cells were detached and incubated with FITC-conjugated Annexin V to stain apoptotic cells and PI to stain necrotic cells. Fluorescence was measured by a FACS Calibur (BD Biosciences) using the FCS Express software package (De Novo Software, Los Angeles, CA).

Proliferation rate was measured using Click-iT 5-ethynyl-2'-deoxyuridine (EdU) cell Proliferation Assay kit (Invitrogen). Briefly, when cells reached 50% confluence, EdU was added to the culture medium at a final concentration of 10 μM and the cells were incubated at 37℃ for 18 h before being fixed with 4% paraformaldehyde. Collected cells were incubated with Click-iT reaction cocktail at room temperature for 30 min. Fluorescence was analyzed by a FACS Calibur (BD Biosciences, San Jose, CA) using the FCS Express software package (De Novo Software, Los Angeles, CA).

miR-486-5p transduction

Passage 1 ADSCs or chondrocytes were transduced with miR-486-5p mimic, miR-486-5p negative control mimic (NC mimic), miR-486-5p inhibitor, and miR-486-5p negative control inhibitor (NC inhibitor) using Lipofectamine™ 2000 according to the manufacturer's instructions. After 24 h of transduction, the cells were used in the following experiments. The sequences were listed below. hsa-miR-486-5p mimics: 5'-UCC UGU ACU GAG CUG CCC CGA G -3'; NC mimics: 5'- UCA CAA CCU CCU AGA AAG AGU AGA -3'; hsa-miR-486-5p inhibitor: 5'- CUC GGG GCA GCU CAG UAC AGG A -3'; NC inhibitor: 5'- UCU ACU CUU UCU AGG AGG UUG UGA -3'.

Exosome isolation and characterization

For exosome isolation, the culture medium of ADSCs was harvested and centrifuged at 2000 g for 30 min first to remove dead cells and debris. The supernatant was filtered through 0.22 μm filter and transferred into a new tube. Total exosome isolation reagent (Invitrogen) was added before centrifuged at 10000 g for 10 min to obtain the exosome samples. Transmission Electron Microscopy was used to observe the exosome morphology and nanoparticle trafficking analysis was used to analyze the size of exos. Exosome markers including CD9 (abcam, ab92726), CD63 (abcam, ab216130), HSP70 (abcam, ab181606) were evaluated using western blot analysis. For the uptake study, exos were incubated with PKH26 (Sigma-Aldrich) for 5 min and resuspended in basal medium before incubated with chondrocytes for 12 h. After that, chondrocytes were fixed and incubated with DAPI for 5 min. Olympus IX51 Inverted Fluorescence

Microscope (Olympus) was used for image capture.

In vitro and in vivo tracking of miR-486-5p

miR-486-5p was tracked in both non-inflammatory and inflammatory [IL-1β (10ng/mL) *in vitro* and destabilization of the medial meniscus (DMM) model *in vivo*] environment. miR-486-5p mimic was labelled with fluorescent dye Cy3 (miR-486-5p-Cy3) and both miR-486-5p-Cy3 transduced ADSCs (miR-486-5p-Cy3 ADSCs) and exos from miR-486-5p-Cy3 ADSCs (miR-486-5p-Cy3 exos) were obtained. In vitro, both normal and IL-1β pre-conditioned chondrocytes were treated with miR-486-5p-Cy3, miR-486-5p-Cy3 ADSCs (in the upper chamber of Transwell culture system) and miR-486-5p-Cy3 exos. After 6 h, 24 h and 7 days, the uptake rate of miR-486-5p-Cy3 was measured using Olympus IX51 Inverted Fluorescence Microscope (Olympus). In vivo, both normal and DMM knee joint were injected with miR-486-5p-Cy3, miR-486-5p-Cy3 ADSCs and miR-486-5p-Cy3 exos. The fluorescent intensity and distribution were measured using IVIS Lumina II in vivo imaging system and Living Image Software (Perkin Elmer) at Day 0, 3 and 7.

Animal model and evaluation

A total of 15 approximately 6 months old Sprague-Dawley rats (300-350g) were used in this study. OA model was established through the transection of medial meniscotibial ligament (DMM). All rats were randomly divided into 5 groups: (1) Negative control group (rats without surgery receiving weekly saline injection into the knee joint); (2)

DMM group (OA model rats receiving weekly saline injection into the knee joint); (3) DMM + miR-486-5p group (OA model rats receiving the weekly injection of 20 ul 10 μg/mL miR-486-5p mimic in PBS into the knee joint); (4) DMM + miR-486-5p ADSCs group (OA model rats receiving the weekly injection of 20 ul $1\times10^{\wedge7}$ miR-486-5p mimic overexpressed ADSCs into the knee joint). (5) DMM + miR-486-5p exos group (OA rats receiving the weekly injection of 20 ul 10 μg/mL exos from miR-486-5p mimic overexpressed ADSCs into the knee joint). Rats were sacrificed 10 weeks after surgery and the knee joints were harvested for evaluation. Knee joints were fixed, decalcified and imbedded in paraffin and cut into 6 μm section. For histological analysis, sections were analyzed using hematoxylin-eosin (HE) staining, safranin-O & fast green staining.

The *in vivo* apoptosis of chondrocytes was assessed using Terminal deoxynucleotidyl transferse dUTP nick end labelling (TUNEL) assay that was performed according to manufacturer's instructions (C1088, Beyotime). Nuclei were stained with DAPI and apoptotic cells were visualized using Olympus IX51 Inverted Fluorescence Microscope (Olympus).

Statistical analysis

Data was presented as mean ± standard deviation (SD). Statistical analysis was performed using SPSS 20.0 software (IBM Corp., NY, USA). The significance of differences between groups was analyzed using Student's t test or one-way *ANOVA*. *P* value < 0.05 was considered significant.

Results

Increased inflammation and ER stress in OA synovium and cartilage

To evaluate the inflammatory and ER stress condition in OA joint, we analyzed the level of several markers in synovium and cartilage. OA synovium demonstrated an increased expression of inflammatory cytokines including IL-1β and TNF-α compared with normal synovium (Fig. 1A). Meanwhile, the expression of proinflammatory M1 macrophage marker iNOS was increased while that of anti-inflammatory M2 macrophage marker CD163 was decreased in OA synovium (Fig. 1A), indicated that synovial macrophage polarized to pro-inflammatory (M1) phenotypes during OA. In line with the inflammatory condition of synovium during OA, an increased level of IL-1β and TNF-α was also observed in OA articular cartilage (Fig. 1B). Previous research showed that inflammatory cytokines could lead to prolonged ER stress in chondrocytes (2), indeed more deposition of ER stress markers including CHOP and GRP78 were found in OA articular cartilage compared with normal articular cartilage (Fig. 1B). These results validated that prolonged ER stress may participated in the progression of OA (19).

ER stress participated in IL-1β induced apoptosis of chondrocytes

To investigate the function of ER stress in chondrocyte apoptosis, ER stress inhibitor 4-PBA was used to treat chondrocytes after IL-1β stimulation. The Annexin-V results indicated that IL-1β could induce apoptosis of chondrocyte, which was largely inhibited by ER stress inhibitor 4-PBA (Fig. 2A). The expression of ER stress marker CHOP in

chondrocytes confirmed that ER stress was elevated after IL-1β stimulation, which could also be downregulated by ER stress inhibitor (Fig. 2B). Western blot further confirmed the involvement of ER stress during IL-1β induced apoptosis of chondrocyte. The expression of ER stress signaling molecules including phosphorylated PERK, phosphorylated IRE1α and GRP78 were increased over IL-1β stimulation, which could be inhibited by 4-PBA treatment (Fig. 2C). Western blot also indicated that the expression of SOX9, a master transcription factor in chondrogenesis, is also downregulated during IL-1β induced apoptosis (Fig. 2C). This downregulation was also rescued by ER stress inhibition (Fig. 2C). The ELISA results demonstrated that IL-1β could stimulate the secretion of other inflammatory cytokines including IL-6 and TNF-α (Fig. 2D), resulting in an inflammatory cascade. In line with declined apoptosis rate, the expression of IL-6 and TNF-α could also be inhibited by 4-PBA treatment (Fig. 2D). These results indicated that ER stress facilitated the inflammation induced apoptosis of chondrocytes.

Characterization of miR-486-5p overexpressing ADSCs and exos

To investigated the role of miR-486-5p in ADSCs, we transduced miR-486-5p mimic, NC mimic, miR-486-5p inhibitor or NC inhibitor into normal ADSCs. The expression of miR-486-5p in ADSCs was evaluated using qPCR after transduction. Compared to NC group, the expression of miR-486-5p was significantly up-regulated in miR-486-5p mimic ADSCs group whereas was down-regulated in miR-486-5p inhibitor transduced group (Fig. 3A). After transduction, exos were isolated and purified from culture media

of each group of ADSCs. qPCR was used to measure the expression of miR-486-5p in five group of exos and a similar trend of miR-486-5p expression was observed as a significant up-regulation in miR-486-5p mimic exos group whereas a significant down-regulation in miR-486-5p inhibitor exos group compared to control exos group (Fig. 3B). We further selected two groups of exos we purified to verify their identity. Scanning electron microscope confirmed the round morphology of exos in NC exos and miR-486-5p mimic exos groups (Fig. 3C). The mean diameter of exos in NC exos and miR-486-5p mimic exos groups were 110.2 and 109.5 nm as measure by NTA system (Fig. 3D). Western blot analysis suggested positive expression of exos markers like CD9, CD63 and HSP70 in both groups (Fig. 3F). Internalization of exos was confirmed, as PKH26 signal was observed in the perinuclear region of PKH26-labelled exos treated chondrocytes in both groups (Fig. 3F).

miR-486-5p exos showed better effect than miR-486-5p on attenuating the ER stress-induced apoptosis in chondrocytes

To investigate the effect of miR-486-5p on the chondrocyte apoptosis, IL-1β pre-conditioned chondrocytes were treated with miR-486-5p, NC mimic exos or miR-486-5p mimic exos. Annexin-V results showed that miR-486-5p treatment could significantly inhibit the ER stress induced apoptosis in IL-1β pre-conditioned chondrocytes (Fig. 4A). Surprisingly, both NC mimic exos and miR-486-5p mimic exos showed better effect on attenuating the ER stress induced apoptosis in IL-1β pre-conditioned chondrocytes, whereas miR-486-5p mimic exos showed a trend of lower

apoptosis rates compared with NC mimic exos (Fig. 4A). The expression of ER stress marker CHOP showed trend of decrement in miR-486-5p group (Fig. 4B). NC mimic exos and miR-486-5p mimic exos both showed greater extent on inhibiting ER stress in chondrocytes than miR-486-5p, among which miR-486-5p mimic exos significantly inhibited the expression of CHOP in IL-1β pre-conditioned chondrocytes (Fig. 4B). Western blot confirmed that apoptosis marker cleaved Caspase-3 and ER stress marker GRP78 showed similar pattern that miR-486-5p mimic exos treatment has the greatest effect on inhibiting apoptosis of chondrocytes (Fig. 4C). miR-486-5p mimic exos treatment also showed the greatest effect on restoring cartilage matrix component type II collagen expression and inhibiting cartilage degradation protease MMP13 expression (Fig. 4C). miR-486-5p mimic exos further reduced the cytokine release of IL-6 and TNF-α in IL-1β pretreated chondrocyte to the lowest level compared with miR-486-5p and NC exos group (Fig. 4D). These results indicated that miR-486-5p containing exos showed better effect than directly administrated miR-486-5p on attenuating the ER stress-induced apoptosis in chondrocytes.

Exosomal miR-486-5p further improved the effect of exos on attenuating the ER stress-induced apoptosis in chondrocytes

We have demonstrated that both NC mimic Exos and miR-486-5p mimic exos could attenuated the ER stress induced apoptosis (Fig. 4). However, we can't rule out the possibility that this effect was solely induced by exos itself rather than miR-486-5p mimic containing exos. To fully validate the therapeutic effect of miR-486-5p mimic

exos on attenuating the ER stress induced apoptosis in chondrocytes, we evaluated the IL-1β pre-conditioned chondrocytes which treated with NC exos, miR-486-5p mimic exos or NC mimic exos. The apoptosis and proliferation rate, ER stress, cartilage matrix related genes and cytokine secretion of chondrocytes were evaluated. As expected, NC exos decreased the apoptosis rate of chondrocytes compared with IL-1β group as shown in Annexin-V result (Fig. 5A). EdU results further confirmed the increased proliferation rate over NC exos treatment as the relative EdU incorporation rate was increased (Fig. 5B). However, the further decreased apoptosis rate (Fig. 5A) and the further increased proliferation rate (Fig. 5B) in miR-486-5p exos group suggested the superiority of miR-486-5p exos over NC exos in apoptosis alleviation and proliferation promotion. Meanwhile, the influence of NC exos on ER stress was further investigated using immunofluorescent staining, as CHOP deposition was decreased by NC exos treatment (Fig. 5C). ER stress was further reduced by miR-486-5p exos demonstrated by an even lower level of CHOP in chondrocytes (Fig. 5C). Western blot showed similar results as the expression of cleaved Caspase 3 and GRP78 were downregulated by exos treatments, in which miR-486-5p exos holds the best effect (Fig. 5D). Cartilage matrix deposition and degradation was measured by qPCR and western blot analyses. qPCR result witnessed an increased expression in cartilage matrix deposition markers *ACAN* and *COL2A1*, and a decreased expression in matrix degradation markers *MMP13* mRNA following NC exos treatment compared with IL-1β group (Fig. 5E). Western blot results further confirmed these conclusions as the expression of type II collagen was increased and MMP13 was decreased

respectively after NC exos administration (Fig. 5E). The IL-1β induced cartilage matrix gene expression changes were also further rescued by miR-486-5p exos treatment, as evidenced by the increased expression of *ACAN, COL2A1* and the decreased expression of *MMP13* mRNA (Fig. 5D), as well as the increased type II collagen and decreased protein level of MMP13 in western blot (Fig. 5D). Meanwhile, the inflammatory cytokine secretion profile rescued by NC exos treatment as the concentration of IL-6 and TNF-α were decreased in ELISA data, was further reduced by miR-486-5p exos treatment (Fig. 5F). Taken together, these results showed that miR-486-5p containing exos showed better effect than normal exos on attenuating the ER stress-induced apoptosis in chondrocytes.

The superiority of miR-486-5p exos over miR-486-5p expressing ADSCs in attenuation of chondrocyte apoptosis in vitro

To illustrate the influence of different administrative methods on the attenuation of chondrocyte apoptosis *in vitro*, miR-486-5p ADSCs and miR-486-5p exos were used to treat IL-1β induced apoptotic chondrocytes. Apparently, both miR-486-5p ADSCs and miR-486-5p exos have inhibitory effect on the apoptosis of chondrocyte as evidenced by the reduced apoptosis rate compared to those in IL-1β group, while miR-486-5p exos showed a trend of better effect (Fig. 6A). Meanwhile, the decreased CHOP deposition in both miR-486-5p ADSCs and miR-486-5p exos groups revealed the inhibited ER stress in IL-1β treated chondrocytes, which was decreased to a lower level in miR-486-5p exos group (Fig. 6B). The downregulated expression of cleaved

Caspase 3 and GRP78 further validated the inhibited apoptosis and ER stress in treatment groups, while miR-486-5p exos showed significantly better effect compared with miR-486-5p ADSCs group (Fig. 6C). Similarly, the increased expression of type II collagen and the decreased expression of MMP13 revealed the remarkably increased chondrogenic matrix deposition in miR-486-5p exos group compared with miR-486-5p ADSCs group (Fig. 6C). Moreover, the increased inflammatory cytokine secretion profile (IL-6 and TNF-α) in IL-1β group was also reversed after miR-486-5p ADSCs and miR-486-5p exos treatment, with the most significant reversal found in miR-486-5p exos group (Fig. 6D). miR-486-5p containing exos showed better effect than miR-486-5p overexpressing ADSCs on attenuating the ER stress-induced apoptosis in chondrocytes.

miR-486-5p tracking in vitro and in vivo

To validated whether the superiority of miR-486-5p mimic exos is due to better delivery, we tracked the sustain of the miR-486-5p under different administrative methods. miR-486-5p-Cy3, miR-486-5p-Cy3 mimic ADSCs, and miR-486-5p-Cy3 mimic exos were obtained and used to treat chondrocytes (miR-486-5p-Cy3 mimic ADSCs were added in the upper chamber of Transwell culture system) in non-inflammatory and inflammatory environments (10 ng/mL IL-1β) for 6 h, 24 h and 7 days. Data witnessed a quick uptake of miR-486-5p-Cy3 by chondrocytes in both miR-486-5p-Cy3 and miR-486-5p-Cy3 exos groups at 6 h (Fig. 7A). After 24 h, the uptake rate in miR-486-5p-Cy3 group increased, whereas was not long-lasting as it dropped after 7 days while

that in miR-486-5p-Cy3 exos group kept endurable, especially with inflammatory stimulation (Fig. 7A). However, the fluorescence was barely detected in chondrocytes with miR-486-5p-Cy3 ADSCs administration at 6 h and 24 h, and a slightly increase of miR-486-5p-Cy3 was witnessed at 7 days even in inflammatory condition (Fig. 7A). In vivo, normal and osteoarthritic knee joint microenvironments (DMM model) were evaluated after the injection of miR-486-5p-Cy3, miR-486-5p-Cy3 ADSCs and miR-486-5p-Cy3 exos. The fluorescent intensity was measured using IVIS Lumina II in vivo imaging system at Day 0, 3 and 7. The results showed no obvious diminishment of fluorescence area and intensity in all three groups after 7 days but only the fluorescence was dispersed towards two directions in miR-486-5p-Cy3 ADSCs group (Fig. 7B). Taken together, miR-486-5p-Cy3 exos group seems to be better delivery method.

The superiority of miR-486-5p exos in cartilage regeneration and inflammation modulation in vivo

To further investigate the effect of different miR-486-5p mimic administration methods on the cartilage regeneration and inflammation modulation, miR-486-5p, miR-486-5p mimic ADSCs and miR-486-5p mimic exos were injected weekly into the DMM joint, respectively. Cartilage and synovium samples were collected and evaluated 10 weeks after DMM. DMM model was successfully built as evidenced by the disorganized chondrocytes and thinning of cartilage in histological staining (Fig. 8A), and increased apoptotic cells in TUNEL analysis (Fig. 8B). All these changes were significantly

reversed by miR-486-5p mimic exos and miR-486-5p mimic ADSCs administration, whereas was slightly reversed by miR-486-5p injection (Fig. 8A, B). miR-486-5p mimic exos treatment showed a trend of lower OARSI score and a significantly lower apoptotic cells rate compared with miR-486-5p mimic ADSCs group (Fig. 8A and 8B). Meanwhile, synovium samples exhibited a pro-inflammatory trend as the increased iNOS and decreased CD163 deposition in the DMM group, which was remarkably reversed by miR-486-5p mimic exos injection, slightly reversed with miR-486-5p mimic ADSCs administration and barely changed with miR-486-5p administration (Fig. 8C). These results further validated the superiority of miR-486-5p mimic exos in attenuating chondrocytes apoptosis and OA progression.

Discussion

Chondrocyte apoptosis is a critical manifestation of the catabolic condition in OA and the inflammatory microenvironment along with ER stress plays an indispensable role in this process. In this study, we demonstrated the therapeutic effect of the miR-486-5p mimic exos in rescuing chondrocytes from the catabolism status *in vitro* and alleviating OA *in vivo*.

In response to the inflammatory environmental stress during OA, chondrocytes shift into a catabolic condition that undergoing apoptosis, matrix degradation and inflammatory cytokine secretion, which were found after Il-1β administration in this study (20). Extracellular matrix of cartilage is composed of structural proteins and proteoglycans, among which type II collagen is an important structural protein (21).

The decreased deposition of type II collagen is indicative of ECM dysregulation during OA progression (22). TNF-α and IL-6 are both pro-inflammatory cytokines that play a critical role in inflammatory response (23). Elevated levels of TNF-α and IL-6 have been found in the synovial fluid, suggesting their crucial role in OA pathogenesis (24). Moreover, TNF-α and IL-6 can induce the production of other cytokines, matrix metalloproteinases (MMPs) and prostaglandins, further inhibit the synthesis of proteoglycans and type II collagen (25). Thus, they play a pivotal role in cartilage matrix degradation and reinforce the vicious cycle in OA (25). Meanwhile, IL-1β successfully induced ER stress activation and chondrocyte apoptosis. Inhibiting ER stress resulting in lower apoptosis rate, which is in alignment with previous studies claiming that ER stress participated in the senescence and apoptosis of OA chondrocytes (2, 26). ER stress is a double-edged sword as its short term activation induces the unfolded protein response (UPR) to restore homeostasis of chondrocytes, but can cause apoptosis if this response is sustained (27). Apparently in our study, inflammatory microenvironment induced sustained ER stress, which further worsens the catabolic status of chondrocytes as the increased apoptosis rate, matrix deterioration and secretion of inflammatory cytokine.

Meanwhile, we identified miR-486-5p to be an important suppressor in the ER stress-induced chondrocyte apoptosis. Previous studies have reported that direct knee joint administration of miR-140 and miR-26a in OA model reduced cartilage injury and synovitis (28, 29). Similarly, in our study, direct administration of miR-486-5p was effective in reversing the catabolic condition of chondrocytes. However, this effect

485 turned out to be limited compared to that of miR-486-5p mimic exos. It is not surprising
486 because some MSCs-derived exos are originally abundant in several specific miRNAs
487 and the delivery of these exos was reported to protect articular cartilage in OA mice
488 (30). Meanwhile, exos contain other bioactive molecules that have a synergistic effect
489 with miRNAs. Indeed, our results showed that exos were equipped with better anti-
490 catabolic ability with miR-486-5p loading. This coincides with previous studies claiming
491 exosomal miR-9-5p (31) and miR-136-5p (32) from bone marrow-derived MSCs are
492 superior than exos alone in cartilage regeneration. This increased therapeutic potential
493 of miRNA packaging exos can be attributed to the definite suppression of one or
494 several of the downstream target molecule. As according to a previous study, Tob1
495 inhibition is the key point in the suppression of rheumatoid arthritis by exosomal miR-
496 486-5p (33), so Tob1 may be one of the targeted molecule of the miR-486-5p exos we
497 analyzed in this study.

498 We also explored whether the administration methods affect the efficiency and
499 effectiveness of miR-486-5p. Both MSCs (34, 35) and their exos (15, 36) are
500 candidates for OA therapy. Exos possess more advantages over MSCs including
501 convenience in storage, stable biological activity, low risk of iatrogenic tumor formation
502 and minimal immunogenicity (37). Previous studies comparing the therapeutic effect
503 on OA and found that exos were superior than their originated MSCs (38). In our study,
504 exos were also found to be a better carrier than ADSCs in miR-486-5p administration
505 for apoptosis alleviation and matrix regeneration of chondrocytes. This result is a little
506 astonishing because we originally believed that miR-486-5p mimic ADSCs are

supposed to secrete miR-486-5p mimic exos. However, the limited miR-486-5p signal in the miR-486-5p mimic ADSCs group chondrocytes is probably due to the poor release of miR-486-5p, as inflammation tends to have a significant impact on the secretome of ADSCs (39).

All our *in vitro* results were mirrored in the *in vivo* study. Firstly, compared with miR-486-5p alone, the administration of miR-486-5p mimic ADSCs resulted in decreased cartilage erosion. Indeed our *in vivo* imaging demonstrated a polarized diffusion signal 7 days after injection, which suggested the migration of ADSCs onto the injured cartilage, as MSCs tend to accumulate in damaged tissue and provides a possible explanation for the superior results for in situ remediation (40). Exos also have a target-homing character (40). Originally, we thought that the administration of MSCs should generate a similar, or even better effect on apoptosis prevention and matrix regeneration because MSCs are supposed to have exosome secretion as well as chondrogenic differentiation and immunoregulatory effect after joint injection. However, our data witnessed an increased deposition of chondroitin sulfate following miR-486-5p mimic exos instead of miR-486-5p mimic ADSCs administration. Similarly, TUNEL data confirmed that an almost vanished deposition of apoptosis signal in both cartilage and subchondral layer with miR-486-5p mimic exos administration, whereas miR-486-5p mimic ADSCs showed lesser effect to rescue the chondrocyte apoptosis in the cartilage layer. We speculated that the potential reason is the rapid elimination of MSCs after joint administration and even if they survived, rarely was there differentiation into the desired cells (41, 42).

Macrophages are immune cells that reside in the synovial lining and can polarize to the pro-inflammatory M1 and the anti-inflammatory M2 phenotypes. Accumulating evidence suggests that the synovial inflammation is correlated with the pathogenesis and progression of OA (43), and research showed that clinical symptoms of OA are correlated with synovial inflammation rather than structural pathology (44). MSCs are susceptive to certain “environmentally responsive” function in the microenvironment (45). Apart from secretion factors, synovial M1 macrophages inhibit chondrogenesis of stem cells while M2 macrophages support the survival of cartilage grafts. In most conditions, MSCs have an anti-inflammatory role to suppress the activation of M1 macrophages and promote M2 polarization *in vitro* (46). However, low levels of inflammatory stimuli can endow MSCs with a pro-inflammatory mode and influence the quality of their secretome (39), which further suggests the necessity of acquiring the secretion products of MSCs before putting in the adverse circumstances. Recent publications have indicated that the anti-inflammatory effects of MSC-derived exos were relied on the transportation of immunoregulatory miRNAs and proteins into inflammatory immune cells, inhibiting the generation of M1 phenotype macrophages and enabling their phenotypic transformation into immunosuppressive M2 macrophages (37). Notably, they have demonstrated the role of ADSC-derived exos on macrophages polarization. Similarly, in our study, treatment with miR-486-5p mimic exos promotes M2 macrophages polarization, contributing to the attenuation of the on-going inflammation, and creates a favorable environment for cartilage regeneration. Interestingly, miR-486-5p mimic exos demonstrated a remarkably increased diffusion

area after 7 days retention, suggesting uptake not only by chondrocytes, but possible uptake by other cell types including synovial cells, which induce widespread anti-inflammation in the joint.

Conclusions

Taken together, these results support the therapeutic role of miR-486-5p mimic exos in inhibiting chondrocytes apoptosis *in vitro* and alleviating OA *in vivo*. Despite the superiority over miR-486-5p and miR-486-5p mimic ADSCs, more critical technological considerations including the route and dose of miR-486-5p mimic exos need to be further explored before clinical applications.

Abbreviations

OA: osteoarthritis; ER: endoplasmic reticulum; miRNAs: microRNAs; ADSCs: adipose derived stem cells; MSCs: mesenchymal stem cells; exos: exosomes; DMM: destabilization of the medial meniscus; TUNEL: terminal deoxynucleotidyl transferse dUTP nick end labelling.

Acknowledgements

The authors would like to thank Translational Medicine Center of the Shanghai East Hospital of Tongji University for help with this study.

Authors' contributions

YW: chondrocytes experiments, data collection and manuscript writing. AF: animal experiments, data analysis and manuscript writing. ZL and LY: human samples collection. LL: hADSCs isolation. ZP, MM and SL: exosomes characterization and isolation. JC and FY: conception and design of the study, and manuscript revising. All authors read and approved the final version of the manuscript.

Funding

This project was sponsored by grants from Shanghai Sailing Program (20YF1440500), the Ministry of Science and Technology of China (2020YFC2002800) and National Natural Science Foundation of China (82002297).

Availability of data and materials

The data that support the findings of this study are available from the corresponding author upon reasonable request.

Declarations

Ethics approval and consent to participate

The study was conducted according to the guidelines of the Institutional Review Boards at Shanghai East Hospital.

Consent for publication

Not applicable.

Competing interests

The authors declare that they have no competing interests.

References

1. Robinson WH, Lepus CM, Wang Q, Raghu H, Mao R, Lindstrom TM, et al. Low-grade inflammation as a key mediator of the pathogenesis of osteoarthritis. Nature reviews Rheumatology. 2016;12(10):580-92.

2. Liu Y, Zhu H, Yan X, Gu H, Gu Z, Liu F. Endoplasmic reticulum stress participates in the progress of senescence and apoptosis of osteoarthritis chondrocytes. Biochem Biophys Res Commun. 2017;491(2):368-73.

3. Liu L, Yan LN, Sui Z. MicroRNA-150 affects endoplasmic reticulum stress via MALAT1-miR-150 axis-mediated NF-kappaB pathway in LPS-challenged HUVECs and septic mice. Life Sci. 2021;265:118744.

4. Kassan M, Vikram A, Li Q, Kim YR, Kumar S, Gabani M, et al. MicroRNA-204 promotes vascular endoplasmic reticulum stress and endothelial dysfunction by targeting Sirtuin1. Sci Rep. 2017;7(1):9308.

5. Li H, Li Z, Pi Y, Chen Y, Mei L, Luo Y, et al. MicroRNA-375 exacerbates knee osteoarthritis through repressing chondrocyte autophagy by targeting ATG2B. Aging (Albany NY). 2020;12(8):7248-61.

6. Li C, Zheng X, Li W, Bai F, Lyu J, Meng QH. Serum miR-486-5p as a diagnostic marker in cervical cancer: with investigation of potential mechanisms. BMC Cancer.

617 2018;18(1):61.
618 7. Jiang M, Li X, Quan X, Yang X, Zheng C, Hao X, et al. MiR-486 as an effective
619 biomarker in cancer diagnosis and prognosis: a systematic review and meta-analysis.
620 Oncotarget. 2018;9(17):13948-58.
621 8. Zhang H, Zhang M, Meng L, Guo M, Piao M, Huang Z, et al. Investigation of key
622 miRNAs and their target genes involved in cell apoptosis during intervertebral disc
623 degeneration development using bioinformatics methods. J Neurosurg Sci. 2020.
624 9. Kong R, Gao J, Si Y, Zhao D. Combination of circulating miR-19b-3p, miR-122-5p
625 and miR-486-5p expressions correlates with risk and disease severity of knee
626 osteoarthritis. Am J Transl Res. 2017;9(6):2852-64.
627 10. Ouboussad L, Hunt L, Hensor EMA, Nam JL, Barnes NA, Emery P, et al. Profiling
628 microRNAs in individuals at risk of progression to rheumatoid arthritis. Arthritis Res
629 Ther. 2017;19(1):288.
630 11. Chai X, Si H, Song J, Chong Y, Wang J, Zhao G. miR-486-5p Inhibits Inflammatory
631 Response, Matrix Degradation and Apoptosis of Nucleus Pulposus Cells through
632 Directly Targeting FOXO1 in Intervertebral Disc Degeneration. Cell Physiol Biochem.
633 2019;52(1):109-18.
634 12. Maheshwari R, Tekade M, Gondaliya P, Kalia K, D'Emanuele A, Tekade RK.
635 Recent advances in exosome-based nanovehicles as RNA interference therapeutic
636 carriers. Nanomedicine (Lond). 2017;12(21):2653-75.
637 13. Toh WS, Lai RC, Hui JHP, Lim SK. MSC exosome as a cell-free MSC therapy for
638 cartilage regeneration: Implications for osteoarthritis treatment. Seminars in cell &

developmental biology. 2017;67:56-64.

14. Stranford DM, Leonard JN. Delivery of Biomolecules via Extracellular Vesicles: A Budding Therapeutic Strategy. Adv Genet. 2017;98:155-75.

15. Zhang S, Chuah SJ, Lai RC, Hui JHP, Lim SK, Toh WS. MSC exosomes mediate cartilage repair by enhancing proliferation, attenuating apoptosis and modulating immune reactivity. Biomaterials. 2018;156:16-27.

16. Zhang S, Chu WC, Lai RC, Lim SK, Hui JH, Toh WS. Exosomes derived from human embryonic mesenchymal stem cells promote osteochondral regeneration. Osteoarthritis and cartilage. 2016;24(12):2135-40.

17. Mao G, Zhang Z, Hu S, Zhang Z, Chang Z, Huang Z, et al. Exosomes derived from miR-92a-3p-overexpressing human mesenchymal stem cells enhance chondrogenesis and suppress cartilage degradation via targeting WNT5A. Stem Cell Res Ther. 2018;9(1):247.

18. Tao SC, Yuan T, Zhang YL, Yin WJ, Guo SC, Zhang CQ. Exosomes derived from miR-140-5p-overexpressing human synovial mesenchymal stem cells enhance cartilage tissue regeneration and prevent osteoarthritis of the knee in a rat model. Theranostics. 2017;7(1):180-95.

19. Hughes A, Oxford AE, Tawara K, Jorcyk CL, Oxford JT. Endoplasmic Reticulum Stress and Unfolded Protein Response in Cartilage Pathophysiology; Contributing Factors to Apoptosis and Osteoarthritis. Int J Mol Sci. 2017;18(3).

20. Zheng L, Zhang Z, Sheng P, Mobasheri A. The role of metabolism in chondrocyte dysfunction and the progression of osteoarthritis. Ageing Res Rev. 2021;66:101249.

661 21. Lefebvre V, Angelozzi M, Haseeb A. SOX9 in cartilage development and disease.
662 Curr Opin Cell Biol. 2019;61:39-47.
663 22. Rahmati M, Nalesso G, Mobasheri A, Mozafari M. Aging and osteoarthritis: Central
664 role of the extracellular matrix. Ageing Res Rev. 2017;40:20-30.
665 23. Wang T, He C. TNF-alpha and IL-6: The Link between Immune and Bone System.
666 Curr Drug Targets. 2020;21(3):213-27.
667 24. Kapoor M, Martel-Pelletier J, Lajeunesse D, Pelletier JP, Fahmi H. Role of
668 proinflammatory cytokines in the pathophysiology of osteoarthritis. Nature reviews
669 Rheumatology. 2011;7(1):33-42.
670 25. Wang T, He C. Pro-inflammatory cytokines: The link between obesity and
671 osteoarthritis. Cytokine Growth Factor Rev. 2018;44:38-50.
672 26. Uehara Y, Hirose J, Yamabe S, Okamoto N, Okada T, Oyadomari S, et al.
673 Endoplasmic reticulum stress-induced apoptosis contributes to articular cartilage
674 degeneration via C/EBP homologous protein. Osteoarthritis Cartilage.
675 2014;22(7):1007-17.
676 27. Hetz C. The unfolded protein response: controlling cell fate decisions under ER
677 stress and beyond. Nat Rev Mol Cell Biol. 2012;13(2):89-102.
678 28. Zhao Z, Dai XS, Wang ZY, Bao ZQ, Guan JZ. MicroRNA-26a reduces synovial
679 inflammation and cartilage injury in osteoarthritis of knee joints through impairing the
680 NF-kappaB signaling pathway. Biosci Rep. 2019;39(4).
681 29. Si HB, Zeng Y, Liu SY, Zhou ZK, Chen YN, Cheng JQ, et al. Intra-articular injection
682 of microRNA-140 (miRNA-140) alleviates osteoarthritis (OA) progression by

683 modulating extracellular matrix (ECM) homeostasis in rats. Osteoarthritis Cartilage.
684 2017;25(10):1698-707.
685 30. Wu J, Kuang L, Chen C, Yang J, Zeng WN, Li T, et al. miR-100-5p-abundant
686 exosomes derived from infrapatellar fat pad MSCs protect articular cartilage and
687 ameliorate gait abnormalities via inhibition of mTOR in osteoarthritis. Biomaterials.
688 2019;206:87-100.
689 31. Jin Z, Ren J, Qi S. Exosomal miR-9-5p secreted by bone marrow-derived
690 mesenchymal stem cells alleviates osteoarthritis by inhibiting syndecan-1. Cell Tissue
691 Res. 2020;381(1):99-114.
692 32. Chen X, Shi Y, Xue P, Ma X, Li J, Zhang J. Mesenchymal stem cell-derived
693 exosomal microRNA-136-5p inhibits chondrocyte degeneration in traumatic
694 osteoarthritis by targeting ELF3. Arthritis Res Ther. 2020;22(1):256.
695 33. Chen J, Liu M, Luo X, Peng L, Zhao Z, He C, et al. Exosomal miRNA-486-5p
696 derived from rheumatoid arthritis fibroblast-like synoviocytes induces osteoblast
697 differentiation through the Tob1/BMP/Smad pathway. Biomater Sci. 2020;8(12):3430-
698 42.
699 34. Matas J, Orrego M, Amenabar D, Infante C, Tapia-Limonchi R, Cadiz MI, et al.
700 Umbilical Cord-Derived Mesenchymal Stromal Cells (MSCs) for Knee Osteoarthritis:
701 Repeated MSC Dosing Is Superior to a Single MSC Dose and to Hyaluronic Acid in a
702 Controlled Randomized Phase I/II Trial. Stem cells translational medicine.
703 2019;8(3):215-24.
704 35. Barry F. MSC Therapy for Osteoarthritis: An Unfinished Story. J Orthop Res.

2019;37(6):1229-35.

36. Zhang S, Teo KYW, Chuah SJ, Lai RC, Lim SK, Toh WS. MSC exosomes alleviate temporomandibular joint osteoarthritis by attenuating inflammation and restoring matrix homeostasis. Biomaterials. 2019;200:35-47.

37. Harrell CR, Fellabaum C, Jovicic N, Djonov V, Arsenijevic N, Volarevic V. Molecular Mechanisms Responsible for Therapeutic Potential of Mesenchymal Stem Cell-Derived Secretome. Cells. 2019;8(5).

38. Zavatti M, Beretti F, Casciaro F, Bertucci E, Maraldi T. Comparison of the therapeutic effect of amniotic fluid stem cells and their exosomes on monoiodoacetate-induced animal model of osteoarthritis. Biofactors. 2020;46(1):106-17.

39. Lee MJ, Kim J, Kim MY, Bae YS, Ryu SH, Lee TG, et al. Proteomic analysis of tumor necrosis factor-alpha-induced secretome of human adipose tissue-derived mesenchymal stem cells. J Proteome Res. 2010;9(4):1754-62.

40. Shi Y, Wang Y, Li Q, Liu K, Hou J, Shao C, et al. Immunoregulatory mechanisms of mesenchymal stem and stromal cells in inflammatory diseases. Nat Rev Nephrol. 2018;14(8):493-507.

41. Wyles CC, Houdek MT, Behfar A, Sierra RJ. Mesenchymal stem cell therapy for osteoarthritis: current perspectives. Stem Cells Cloning. 2015;8:117-24.

42. Liu S, Liu D, Chen C, Hamamura K, Moshaverinia A, Yang R, et al. MSC Transplantation Improves Osteopenia via Epigenetic Regulation of Notch Signaling in Lupus. Cell Metab. 2015;22(4):606-18.

43. Zhang H, Lin C, Zeng C, Wang Z, Wang H, Lu J, et al. Synovial macrophage M1

polarisation exacerbates experimental osteoarthritis partially through R-spondin-2. Ann Rheum Dis. 2018;77(10):1524-34.

44. Shu CC, Zaki S, Ravi V, Schiavinato A, Smith MM, Little CB. The relationship between synovial inflammation, structural pathology, and pain in post-traumatic osteoarthritis: differential effect of stem cell and hyaluronan treatment. Arthritis Res Ther. 2020;22(1):29.

45. Murphy MB, Moncivais K, Caplan AI. Mesenchymal stem cells: environmentally responsive therapeutics for regenerative medicine. Exp Mol Med. 2013;45:e54.

46. Harrell CR, Markovic BS, Fellabaum C, Arsenijevic A, Volarevic V. Mesenchymal stem cell-based therapy of osteoarthritis: Current knowledge and future perspectives. Biomed Pharmacother. 2019;109:2318-26.

Figure legends

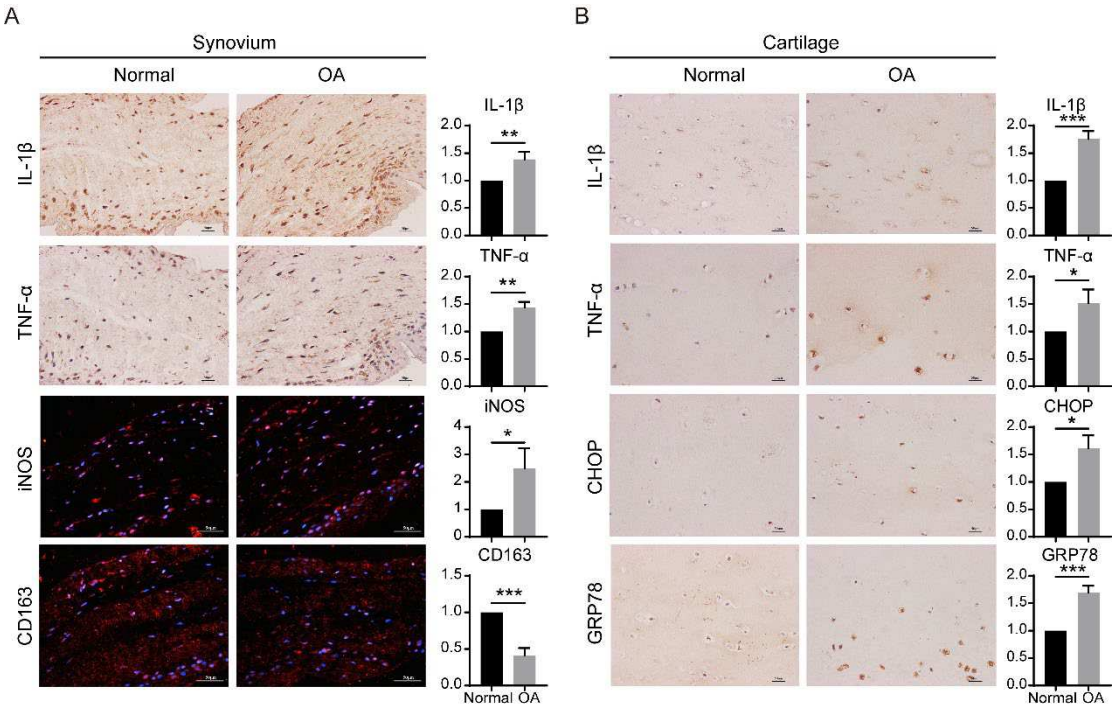

Fig. 1 Evaluation of inflammation and ER stress in normal and OA synovium and

cartilage. (A) Immunohistochemical and immunofluorescent staining of inflammatory cytokines IL-1β and TNF-α, M1 macrophage marker iNOS and M2 macrophage marker CD163 in normal and OA synovium samples. (B) Immunohistochemical staining of IL-1β, TNF-α and ER stress markers CHOP and GRP78 in normal and OA articular cartilage samples. The statistical significance was assessed using two-tailed Student's unpaired t tests. Data represent mean ± SD (*p<0.05, **p < 0.01, ***p < 0.001).

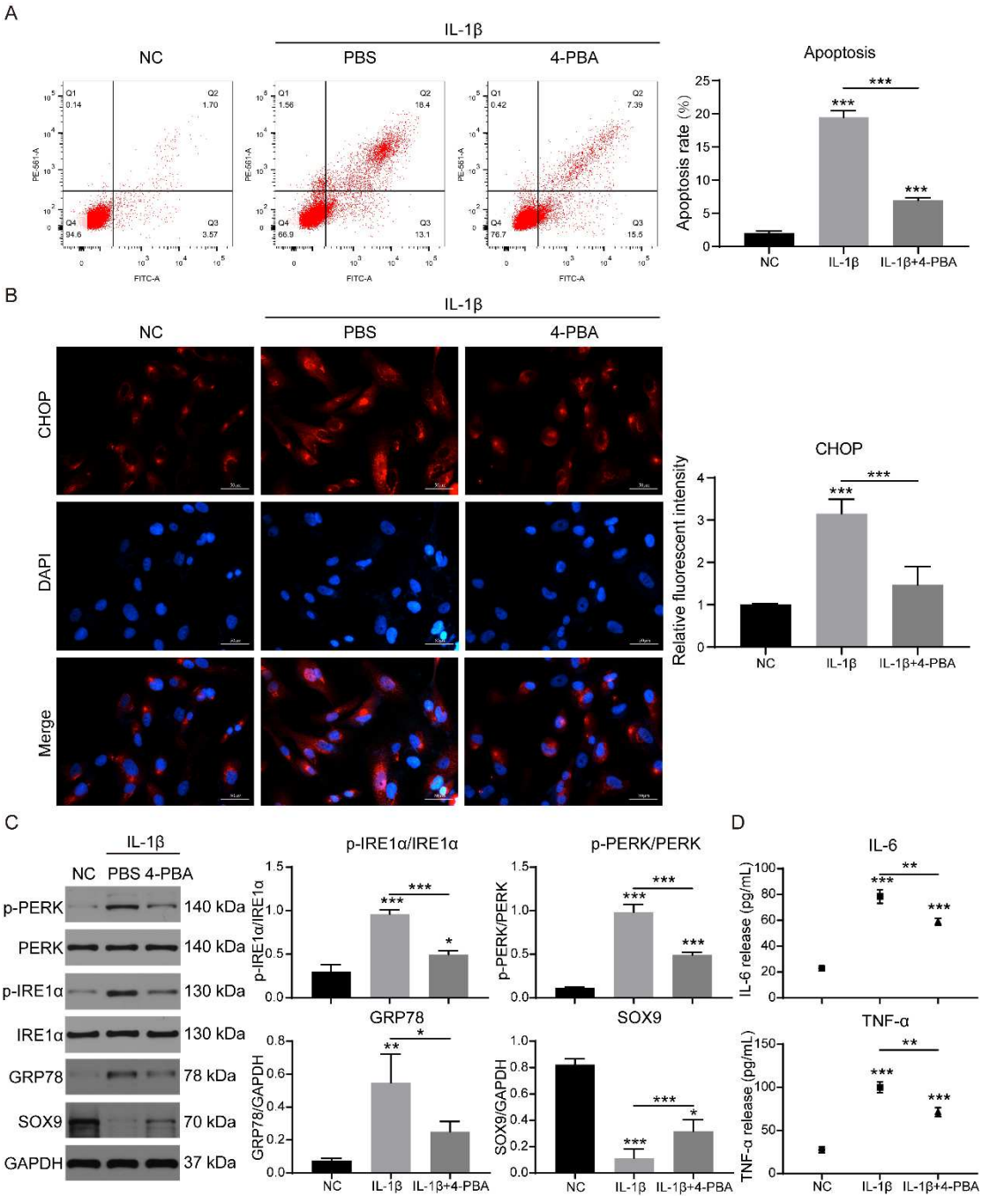

Fig. 2 Role of ER stress on IL-1β-induced apoptosis of chondrocytes. Chondrocytes (NC group) were treated with 10 ng/mL IL-1β (IL-1β group) or IL-1β + ER stress inhibitor 4-PBA (4-PBA group). (A) The apoptosis rate was evaluated using Annexin-V Staining. (B) The expression of CHOP was evaluated using immunofluorescent staining. (C) The expression of p-PERK, PERK, p-IRE1α, IRE1α, GRP78 and SOX9 were evaluated using Western Blot. GAPDH served as internal

control. (D) The concentration of IL-6 and TNF-α in the culture medium were evaluated using ELISA. The statistical significance was assessed using one-way ANOVAs with Tukey's multiple comparison tests. Data represent mean ± SD (*p<0.05, **p < 0.01, ***p < 0.001).

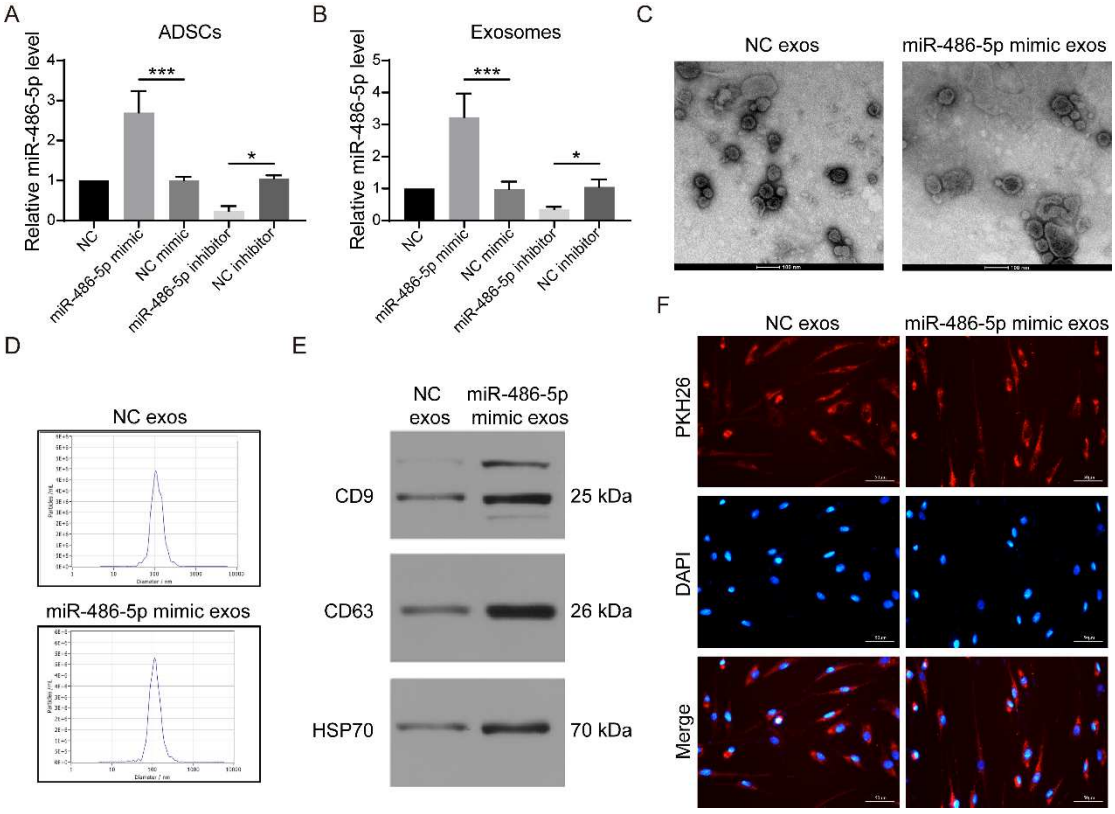

Fig. 3 Characterization of miR-486-5p transfected ADSCs and exos. miR-486-5p mimic, negative control mimic (NC mimic), miR-486-5p inhibitor and NC inhibitor were transfected into normal ADSCs (NC group) before exos were obtained from the corresponding group of ADSCs. The expression of miR-486-5p in ADSCs (A) and the corresponding exos (B) were evaluated. (C) Scanning Electron Microscope was used to observe exos from NC group ADSCs (NC exos) and miR-486-5p mimic transfected ADSCs (miR-486-5p exos). (D) The diameter of exos was determined using Nanoparticle Tracking Analysis (NTA). (E) The expression of exosome markers CD9,

CD63 and HSP70 in exos were determined using western blot. (F) The uptake of exosome by chondrocytes was determined using PKH26 staining. The statistical significance was assessed using one-way ANOVAs with Tukey's multiple comparison tests. Data represent mean ± SD (*p<0.05, ***p < 0.001).

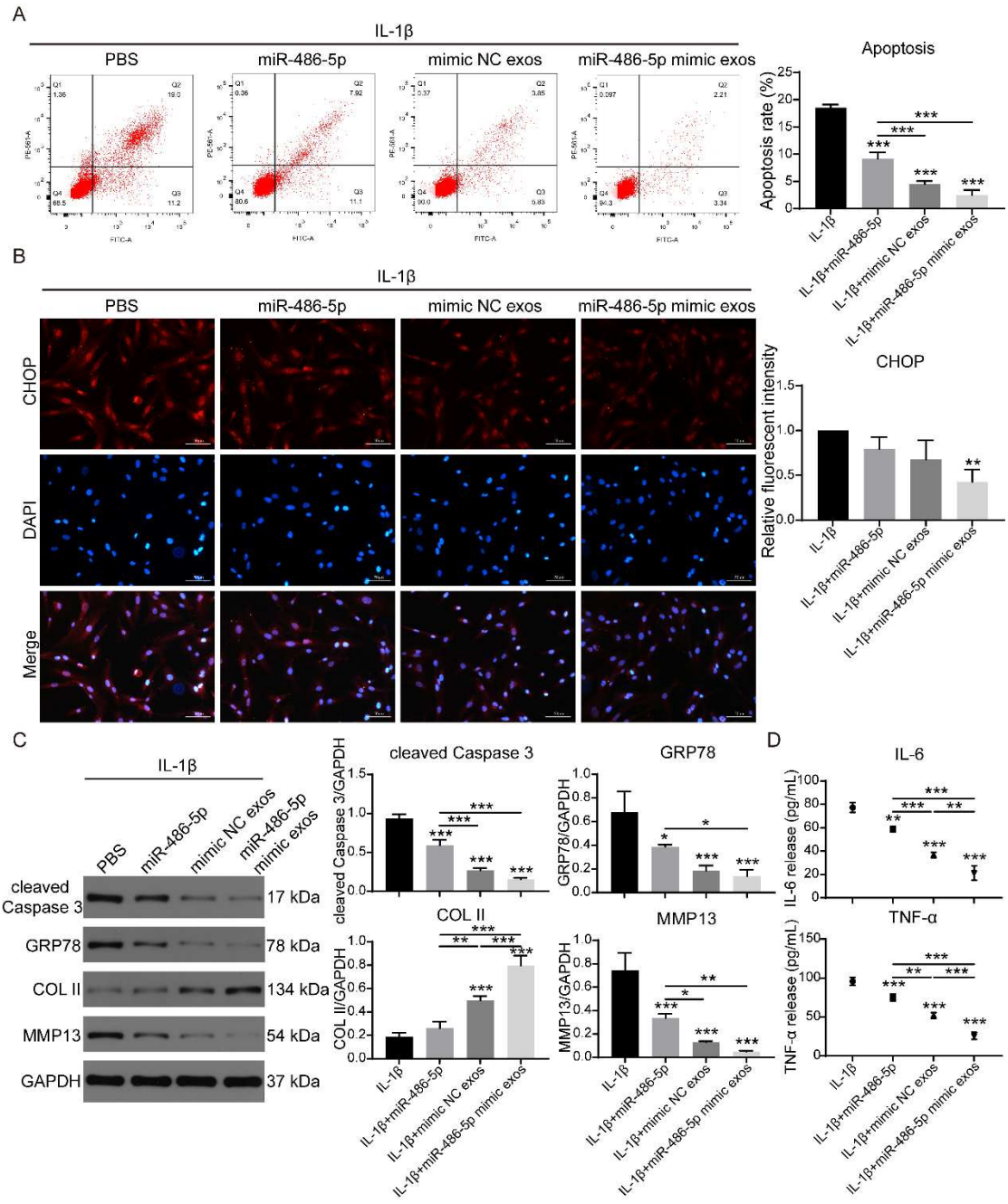

Fig. 4 Comparation of miR-486-5p and exosomal miR-486-5p on ER stress and apoptosis of chondrocytes. Chondrocytes were treated with 10 ng/mL IL-1β (IL-1β

775 group), IL-1β + miR-486-5p mimic (miR-486-5p group), IL-1β + exos from miR-486-5p
776 mimic NC transfected ADSCs (miR-486-5p NC exos group) and IL-1β + exos from
777 miR-486-5p mimic transfected ADSCs (miR-486-5p exos group). (A) The apoptosis
778 rate of each group was evaluated using Annexin-V Staining. (B) The expression of
779 CHOP of each group was evaluated using immunofluorescent staining. (C) The
780 expression of cleaved Caspase-3, GRP78, type II collagen and MMP-13 were
781 evaluated using Western Blot. GAPDH served as internal control. (D) The
782 concentration of IL-6 and TNF-α were evaluated using ELISA. The statistical
783 significance was assessed using one-way ANOVAs with Tukey's multiple comparison
784 tests. Data represent mean ± SD (*$p<0.05$, **$p < 0.01$, ***$p < 0.001$).

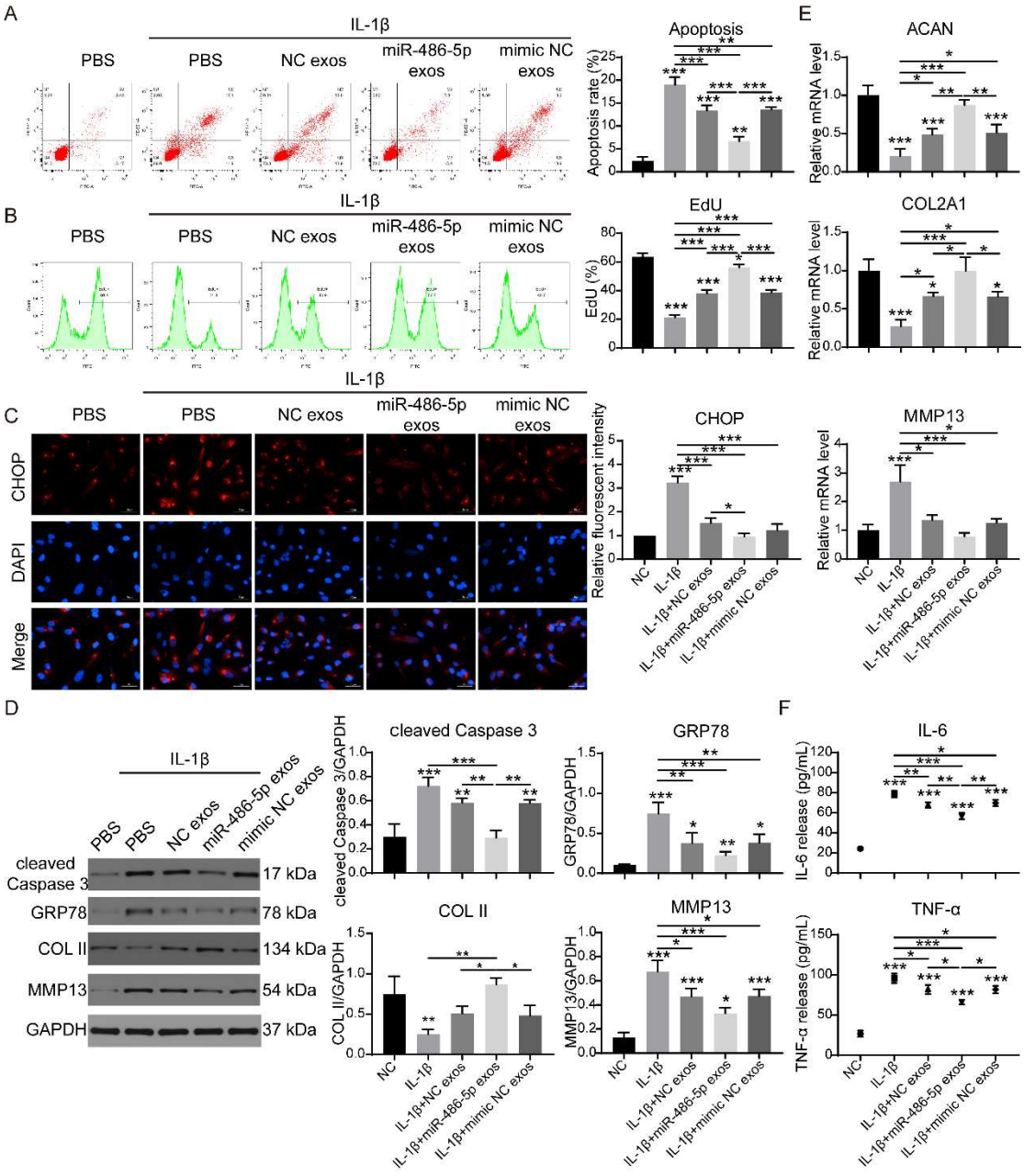

785

786 **Fig. 5 Comparation of exosomes and miR-486-5p packaging exosomes on ER**

787 **stress and apoptosis of chondrocytes.** Chondrocytes (NC group) were treated with

788 10 ng/mL IL-1β (IL-1β group), IL-1β + ADSCs derived exos (NC exos group), IL-1β +

789 exos from miR-486-5p mimic transfected ADSCs (miR-486-5p exos group) and IL-1β

790 + exos from miR-486-5p mimic NC transfected ADSCs (miR-486-5p NC exos group).

791 (A) The apoptosis rate of each group was evaluated using Annexin-V staining. (B) The

792 proliferation rate of each group was evaluated using Click-iT® EdU assay. (C) The

expression of CHOP was evaluated using immunofluorescent staining. (D) The expression of cleaved Caspase-3, GRP78, type II collagen and MMP-13 were evaluated using Western Blot. GAPDH served as internal control. (E) The expression of mRNA *ACAN*, *COL2A1* and *MMP13* of each group were evaluated. (F) The concentration of IL-6 and TNF-α in culture media were evaluated using ELISA. The statistical significance was assessed using one-way ANOVAs with Tukey's multiple comparison tests. Data represent mean ± SD (*p<0.05, **p < 0.01, ***p < 0.001).

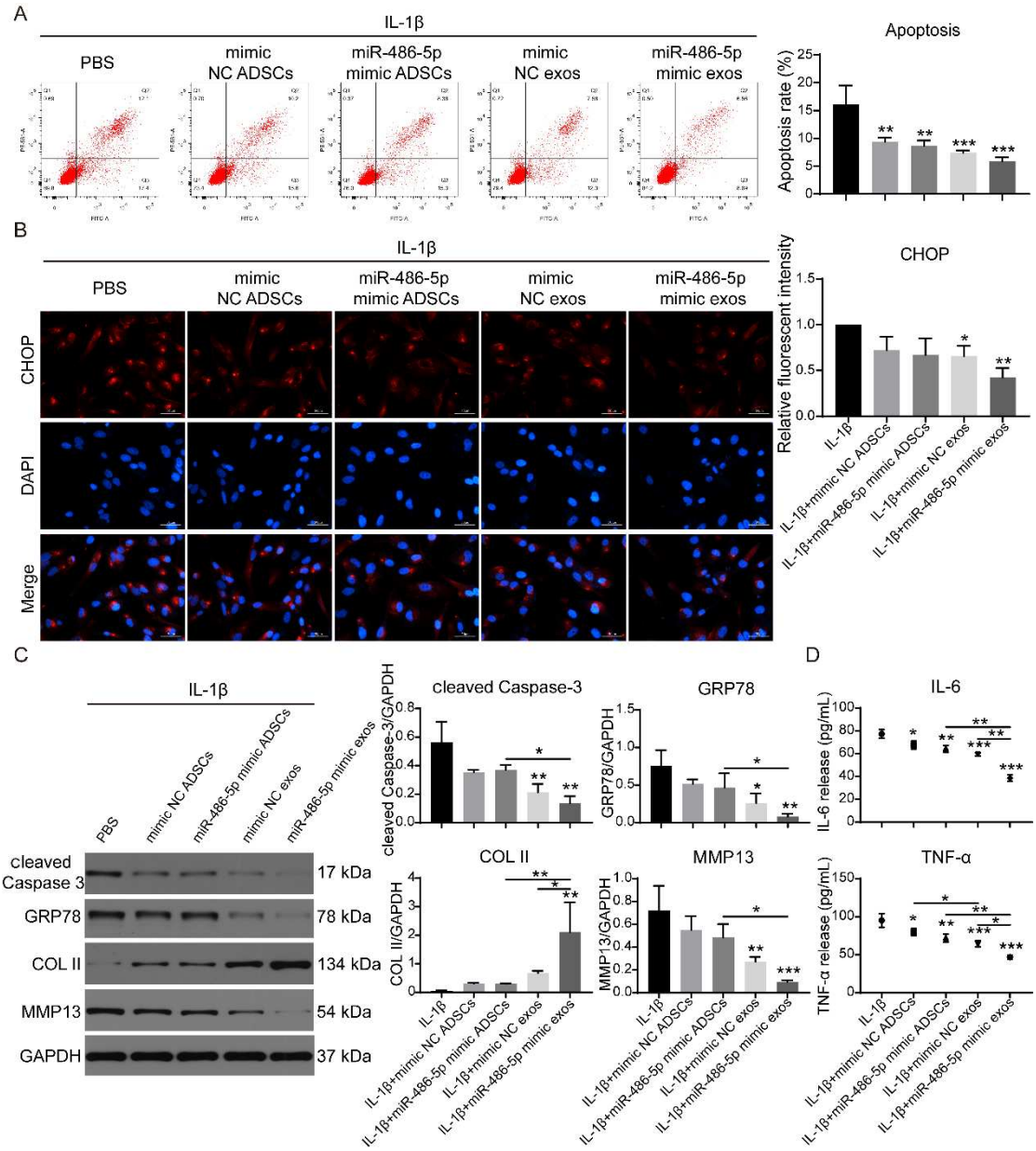

Fig. 6 Comparation of exosomal miR-486-5p over miR-486-5p overexpressing ADSCs on ER stress and apoptosis of chondrocytes. Chondrocyte were treated with 10 ng/mL IL-1β (IL-1β group), IL-1β + miR-486-5p mimic NC transfected ADSCs (mimic NC ADSCs group), IL-1β + miR-486-5p mimic transfected ADSCs (miR-486-5p mimic ADSCs group), IL-1β + exos from miR-486-5p mimic NC transfected ADSCs (mimic NC exos group) and IL-1β + exos from miR-486-5p mimic transfected ADSCs (miR-486-5p mimic exos group). (A) The apoptosis rate of each group was evaluated using Annexin-V Staining. (B) The expression of CHOP of each group was evaluated using immunofluorescent staining. (C) The expression of cleaved Caspase-3, GRP78, type II collagen and MMP-13 were evaluated using Western Blot. GAPDH served as internal control. (D) The concentration of IL-6 and TNF-α in culture media were evaluated using ELISA. The statistical significance was assessed using one-way ANOVAs with Tukey's multiple comparison tests. Data represent mean ± SD (*$p<0.05$, **$p < 0.01$, ***$p < 0.001$).

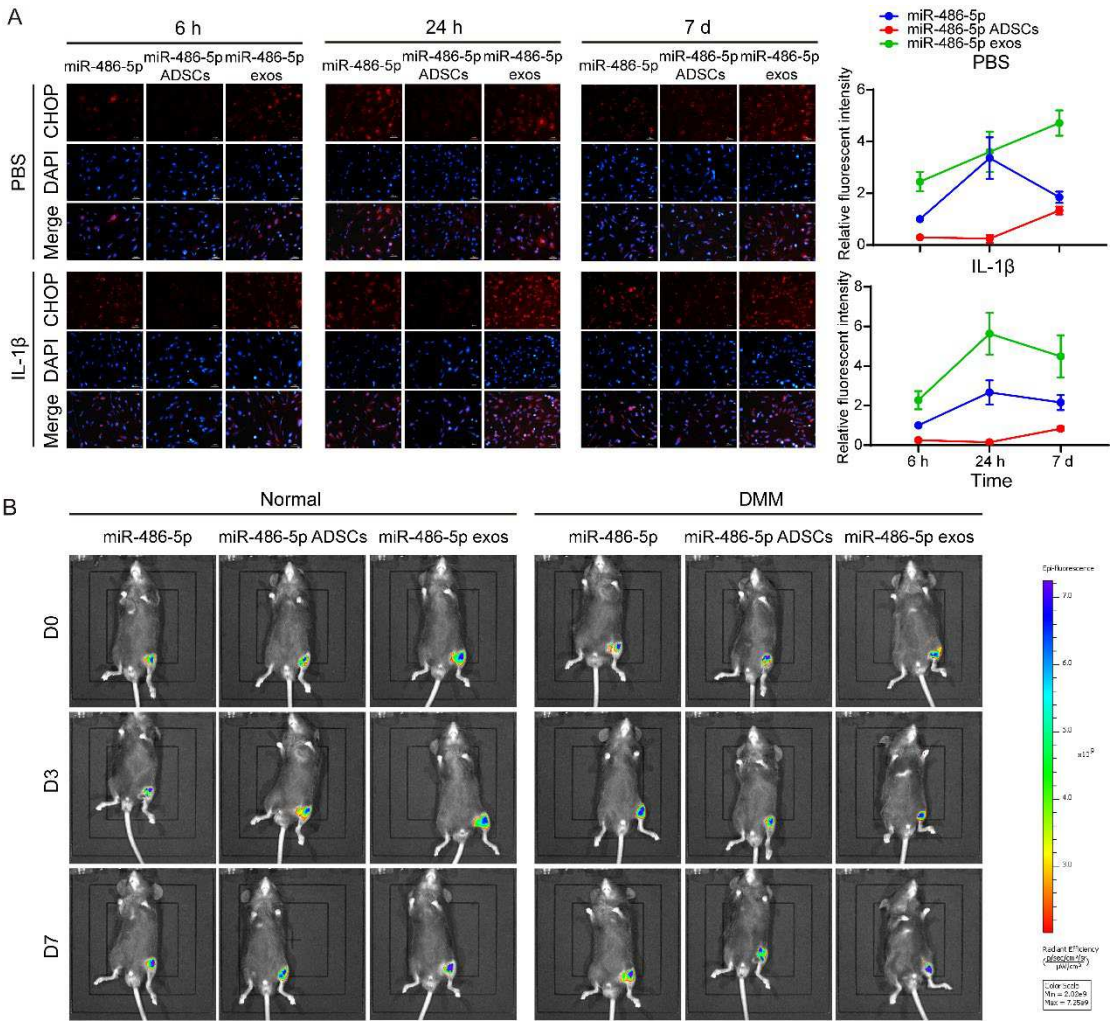

Fig. 7 Tracking of different miR-486-5p administrative methods *in vitro* and *in vivo*. miR-486-5p was labeled with fluorescent dye Cy3 (miR-486-5p-Cy3) and miR-486-5p-Cy3 transfected ADSCs (miR-486-Cy3 ADSCs), and exos from miR-486-5p-Cy3 transfected ADSCs (miR-486-Cy 3 exos) were obtained. (A) *In vitro*, non-inflammatory and inflammatory environments (10 ng/mL IL-1β) were created for chondrocytes before they were treated with miR-486-5p-Cy3, miR-486-5p-Cy3 ADSCs and miR-486-5p-Cy3 exos. After 6 h, 24 h and 7 days, the uptake rate of miR-486-5p-Cy3 was measured using fluorescent staining. (B) *In vivo*, non-inflammatory and inflammatory knee joint micro-environments (DMM) were created before injection with miR-486-5p-Cy3, miR-486-5p-Cy3 ADSCs and miR-486-5p-Cy3 exos. The fluorescent

intensity was measured using IVIS Lumina II *in vivo* imaging system at Day 0, 3 and 7.

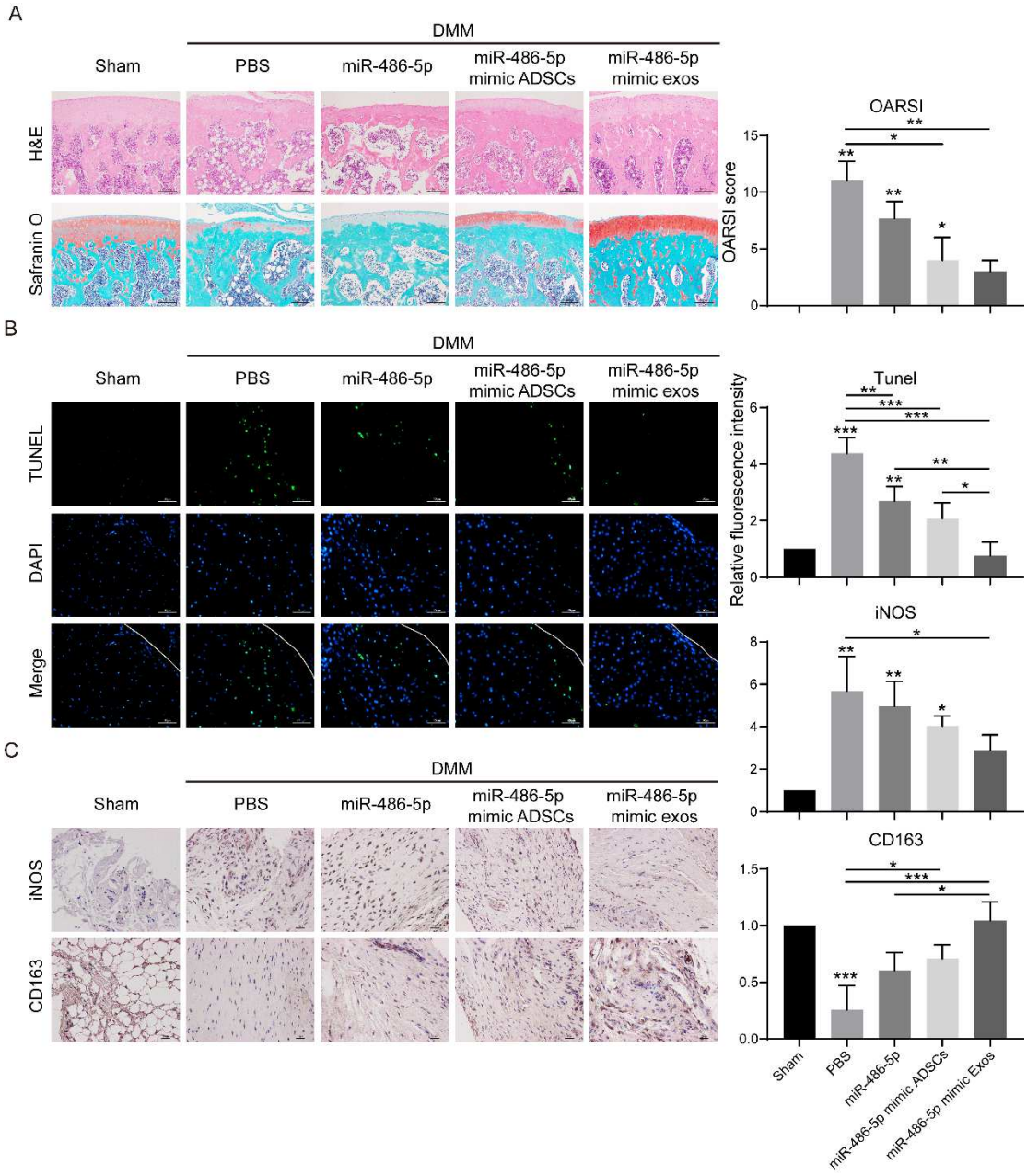

Fig. 8 *In vivo* effect of different miR-486-5p administrative methods in OA mice model. OA model (DMM) was set up and miR-486-5p mimic (miR-486-5p group), miR-486-5p transfected ADSCs (miR-486-5p mimic ADSCs group), and exos from miR-486-5p transfected ADSCs (miR-486-5p mimic exos group) were injected into the knee joint of normal and OA mice. Joint and synovium samples were collected after 10 weeks. (A) Hematoxylin-eosin (H&E) and safranin O/fast green were used to evaluate

834 the matrix deposition and cartilage erosion of joint samples. (B) TUNEL assay were
835 used to evaluate the apoptosis condition of joint samples. (C) Immunohistochemical
836 staining of iNOS and CD163 were used to evaluate the polarization of macrophages
837 in synovium samples.
838